Transportation Geotechnics 1 (2014) 91–105

Contents lists available at ScienceDirect

Transportation Geotechnics

journal homepage: www.elsevier.com/locate/trgeo

Investigation of interlayer soil behaviour by field monitoring

Yu-Jun Cui [a,*], Francisco Lamas-Lopez [a,b], Viet Nam Trinh [a,c], Nicolas Calon [b], Sofia Costa D'Aguiar [b], Jean-Claude Dupla [a], Anh Minh Tang [a], Jean Canou [a], Alain Robinet [b]

[a] Laboratoire Navier/CERMES, Ecole des Ponts ParisTech (ENPC), 6 et 8 avenue Blaise Pascal, Cité Descartes, Champs-sur-Marne, 77455 Marne-la-Vallée cedex 2, France
[b] Société Nationale des Chemins de Fer (SNCF), 6 avenue François Mitterrand, 93574 La Plaine Saint Denis cedex, France
[c] Systra, 72 rue Henry Farman, 75015 Paris, France

ARTICLE INFO

Article history:
Received 3 February 2014
Revised 14 April 2014
Accepted 29 April 2014
Available online 2 June 2014

Keywords:
Moulin Blanc site
Evaporation
Accelerometer
Double integration
Particle displacement

ABSTRACT

As opposed to the new ballasted railway tracks where a sub-ballast layer is often emplaced, the conventional railway tracks were constructed with ballast directly emplaced on the natural sub-soils. Thereby, a layer of mixed materials, namely interlayer, was formed over time mainly by interpenetration between ballast and sub-soils. As this layer plays an important role in transmitting load to the sub-soils, its behaviour under the effects of dynamic loading and climate changes is of primary importance for the stability of tracks. In order to understand the behaviour of the material in such interlayers, field monitoring was performed at a selected site in France, namely Moulin Blanc. Firstly, site investigation was done by borehole, allowing the interlayer location to be identified. Secondly, the interlayer was instrumented with suction probes, temperature sensors and accelerometers at different depths. Two piezometers were also installed for water table monitoring, and a weather station was installed for air data monitoring. The data recorded allowed the suction changes with water evaporation and the behaviour of tracks under the effect of temperature to be analysed. Moreover, the recorded data of acceleration allowed assessing the double-integration method for different kinds of train. It was observed that the site is out of the hazards related to freeze/thaw and the double-integration method can be applied to determine the particle velocity and displacement provided that appropriate filters are used. Note however that further study is needed to confirm this point with comparison between the measured particle displacement and the calculated one.

Introduction

In France, most railway tracks are ballasted and the whole network is composed of new lines for high velocity trains and conventional lines for other categories. In the case of new lines, a sub-ballast is placed between ballast and sub-grade (SNCF Direction de l'Ingénierie, 2006). This sub-layer has the main functions of (i) ensuring the relatively uniform force transmission to the sub-structure, (ii) ensuring the grain size transition from ballast to sub-structure, (iii) protecting sub-structure from excessive water infiltration and (iv) protecting the sub-structure against frost. As opposed to the new lines, the conventional lines have their ballast directly placed on the sub-grade. Under the effect of train circulation over time, an interlayer was created mainly by interpenetration between subgrade soils and ballast. This layer has been found to be well "compacted" by train circulation over long time: the in-situ dry density can be as high as 2.4 Mg/m^3 (Trinh et al.,

* Corresponding author. Address: Ecole des Ponts ParisTech, 6-8 av. Blaise Pascal, Cité Descartes, Champs-sur-Marne, F-77455 MARNE LA VALLEE, France. Tel.: +33 1 64 15 35 50; fax: +33 1 64 15 35 62.
E-mail address: yujun.cui@enpc.fr (Y.-J. Cui).

http://dx.doi.org/10.1016/j.trgeo.2014.04.002
2214-3912/

2011). Thereby, mechanically it consists of a good bearing layer in the sub-structure. This is why this layer is kept in the French conventional track renewal programme. Note that this track renewal program is important because it almost involves the whole French network: the conventional lines represent 94% of a whole network of about 30,000 km. Fig. 1 illustrates the difference between the new and conventional lines.

As the interlayer was formed naturally, it can contain significant amount of fines. Fig. 2 shows a comparison of grain size distribution between sub-ballast and the interlayer soil taken at the site of Sénissiat (North–West of Lyon, France). Note that for the sub-ballast a range of variations is presented. It can be observed that the main difference between the sub-ballast and the interlayer soil lies in the fines content: there are no grains smaller than 0.1 mm in sub-ballast whereas the fraction of grains smaller than 0.1 mm can reach 20% in the interlayer soil. Due to the presence of fines in the interlayer, the hydro-mechanical behaviour of the interlayer soil can be greatly affected by the sensitivity of the fines to changes in water content. Thereby, when renewing the conventional tracks to fulfil the requirements in terms of increase of load and velocity of train, it is important to take this sensitivity into account.

This sensitivity was investigated in the laboratory in terms of hydraulic behaviour (Cui et al., 2013; Duongt et al., 2013) and mechanical behaviour (Trinh et al., 2011, 2012; Duongt et al., 2013) for the interlayer soil taken from Sénissiat. It has been observed that the hydraulic conductivity of this soil is mainly governed by the suction inside the fines, the coarse elements being inert for the water transfer. The mechanical behaviour has been found to be strongly dependent on the water and fines contents: under cyclic loading, the higher the fines content the larger the permanent axial strain in the case of high water content. However, an opposite trend was identified in the case of low water content: adding fines decreased the permanent axial strain.

The hydro-mechanical sensitivity of interlayer soil was also investigated in field conditions at a site instrumented with weather station, accelerometers, suction probes, temperature sensors and piezometres. In this paper, the results obtained are presented, including the site characterisation, the site instrumentation, the evaporation rate deduced from the climate data, the soil suction and temperature

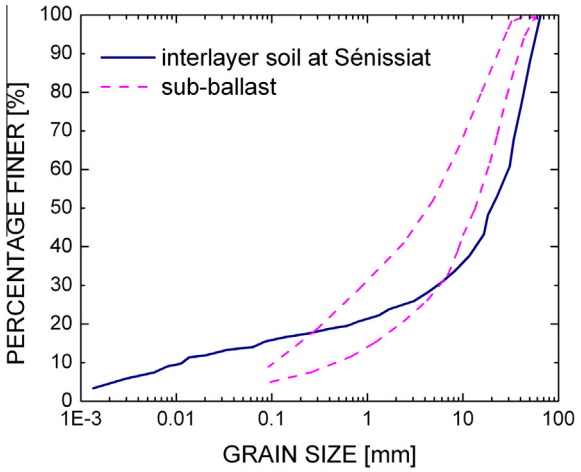

Fig. 2. Comparison of grain size distribution between sub-ballast and interlayer soil.

changes, as well as the assessment of the double integration method for particle displacement determination based on the accelerometer data.

Site characterisation

The experimental site is located in the region of Nord-Pas de Calais, France, in the middle of the 'Douai – Valenciennes' line that was constructed in the late XIXth century. This site is in a cutting zone, and was instrumented at kilometre 230 + 400 of the line number 262,000 of the French railway network. Different trains are involved: High velocity (TGV), Intercity (TER) and Freight. The train velocity at the site is limited to 110 km/h.

For the purpose of site characterisation, soil sampling was done in different locations in the zone from kilometre 230 + 000 to kilometre 231 + 000. Different soils were identified, in particular the interlayer soil of black colour (see Fig. 3a and b) and the sub-soil in yellow colour (see Fig. 3b). For each borehole, the depth was determined using a ruler as shown in Fig. 3c.

Fig. 4 shows the soil profile in the studied section. The thickness of the ballast layer is about 50 cm, with about 30 cm fresh ballast and 20 cm fouled ballast. The interlayer

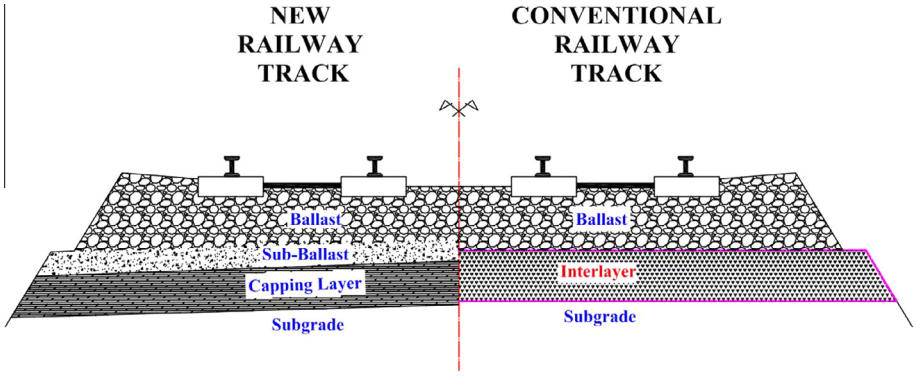

Fig. 1. Comparison between new and conventional railway tracks.

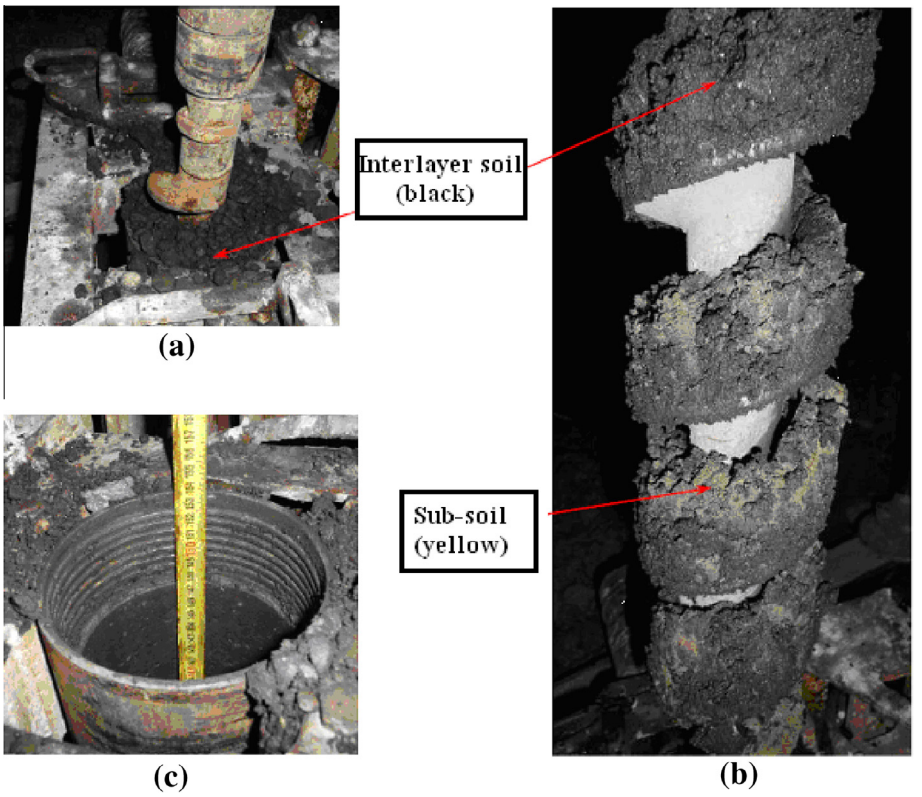

Fig. 3. Site characterisation by sampling.

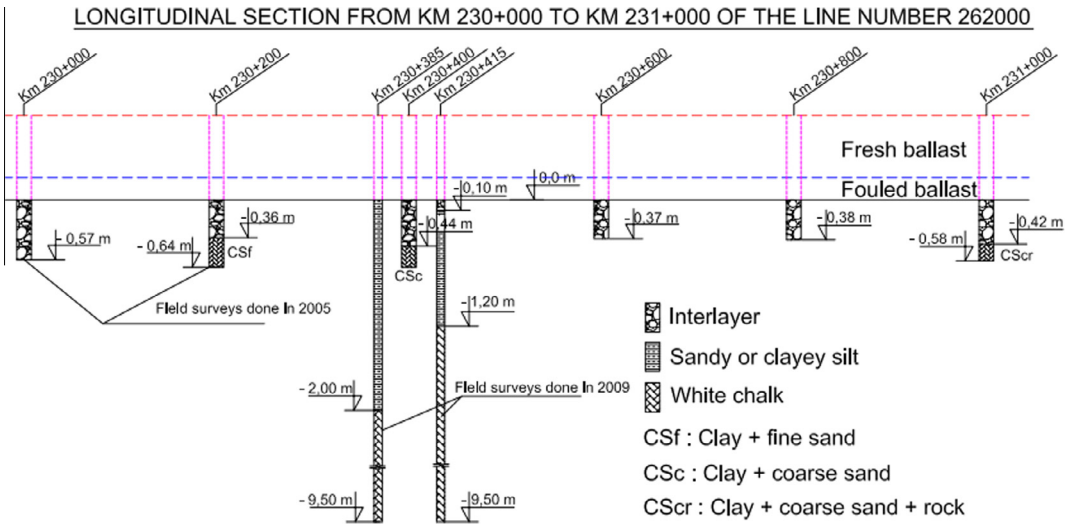

Fig. 4. Soil profile at Moulin Blanc site.

thickness varied from 10 to 57 cm. The subgrade consists of either sandy or clayey silt, with the presence of chalk and clay mixed with sand and rock in some locations.

Site instrumentation

The field instrumentation was done at kilometre 230 + 400 of the line. Based on the site characterisation, it was decided to instal the suction/temperature probes at −0.20, −0.30 and −0.50 m depths under the ballast layer in two zones A and B, at 20 m distance from each other (see Fig. 5a). Two other suction/temperature probes were installed in a zone out of tracks (zone C) and at −0.30 and −0.50 m depths. A temperature sensor was installed at the platform surface in zone C (see Fig. 5a). A total of 8 suction probes and 9 temperature sensors were installed.

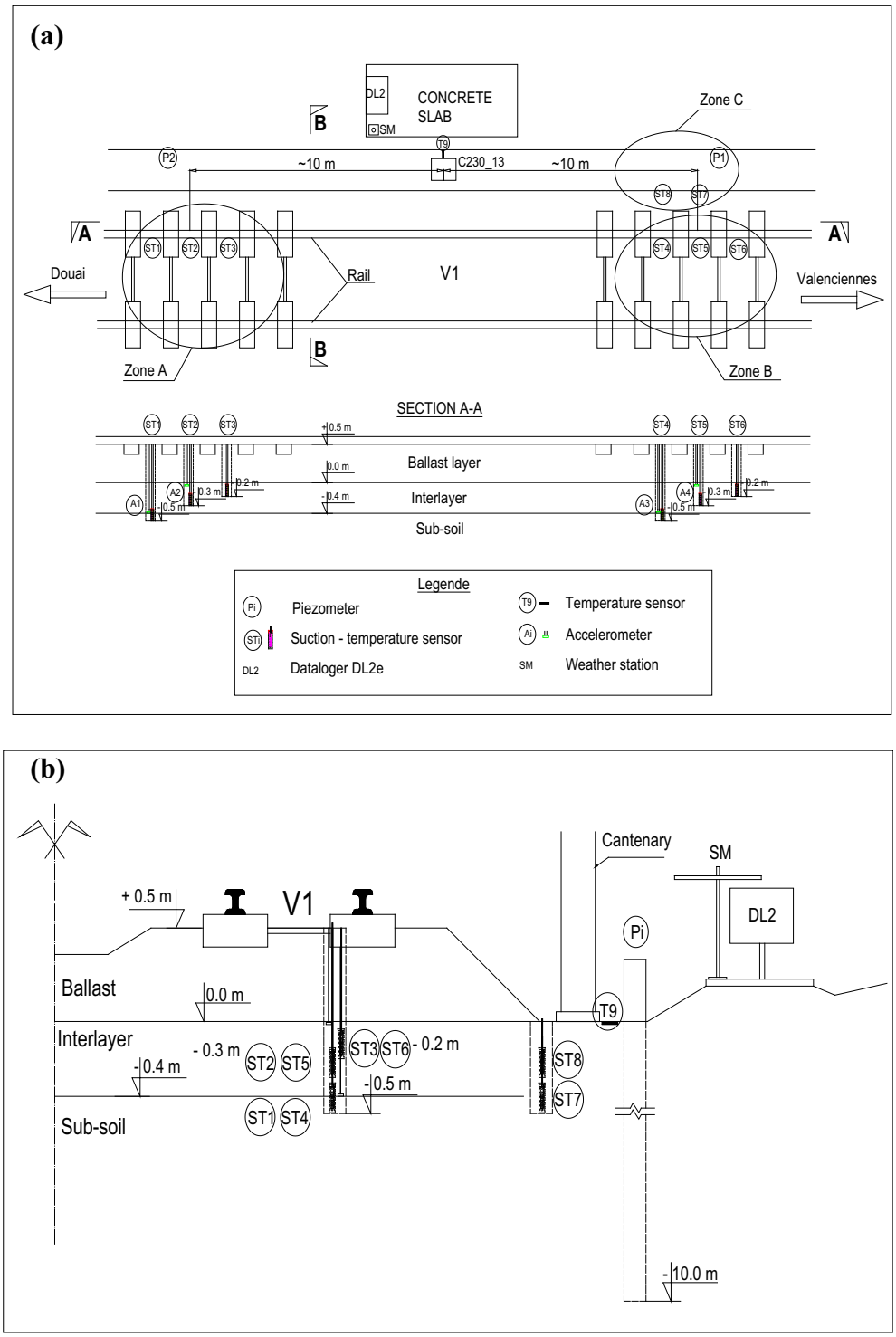

Fig. 5. Site instrumentation. (a) Longitudinal section; (b) Transversal section.

A weather station was installed on the excavation slope to monitor solar radiation, air temperature, air humidity and rainfall (see Fig. 5b). Two piezometres of 10 m depth each were installed near zone A and zone B respectively for the water table monitoring.

Four piezo-electric accelerometers ICP/PCB-601A12 were used, with a measurement range of ±10 g, a frequency ranging from 0.47 to 4000 Hz and a resonant frequency of 16,000 Hz. Two were implemented in zone A at −0.10 and −0.40 m depths respectively, and two

others in zone B at −0.10 and −0.40 m depths, respectively (see Fig. 5). Moreover, strain gauges were glued on the rail for the measurement of rail strain under the passages of trains.

Fig. 6 shows the operation sequence adopted for the installation of sensors beneath the ballast layer. A metal tube (Φ = 9 cm, L = 100 cm) was first installed over the whole height of ballast layer (Fig. 6a). Pre-drilling was then preformed using an auger until the desired depth, with excavated soils collected (Fig. 6b). At the desired depth, the suction/temperature probes and accelerometers were installed while keeping the metal tube in place (Fig. 6c). The borehole was back-filled with the excavated soil (Fig. 6d) by compaction (Fig. 6e). Finally, the metal tube was removed and the ballast layer was completed (Fig. 6f).

Fig. 7 shows a photograph of the instrumented site, where the 3 zones – A, B and C, a piezometre, the weather station and the datalogger can be identified.

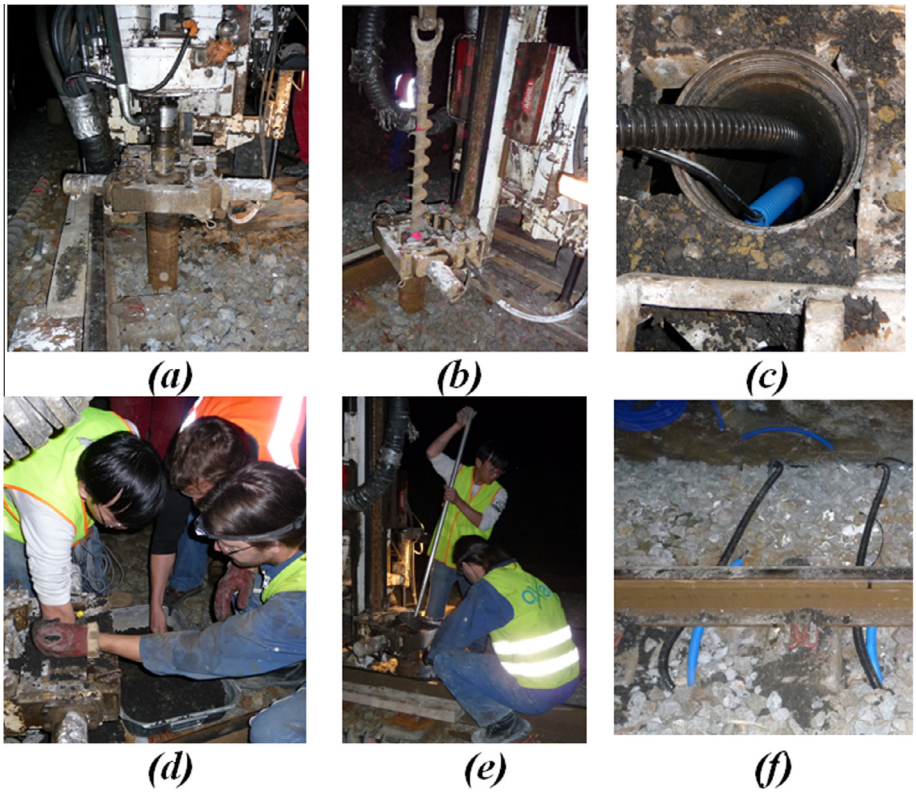

Fig. 6. Operation sequence of instrumentation. (a) Insertion of a metal tube over height of ballast layer; (b) pre-drilling; (c) implementation of sensors; (d) back-filling the borehole; (e) soil compaction; (f) removing the metal tube and completing the ballast layer.

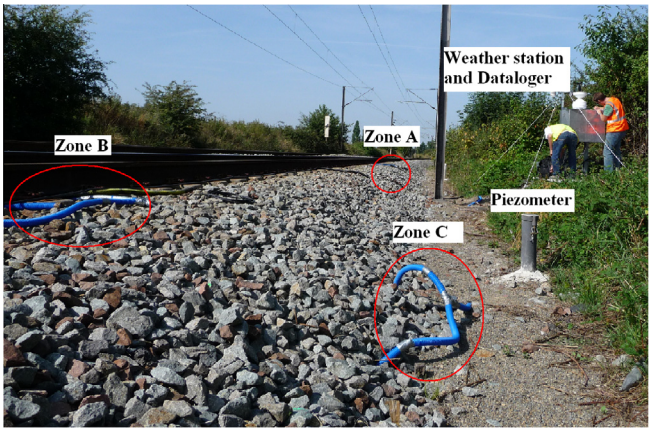

Fig. 7. An overall view of the instrumented site.

Climatic records and soil temperature/suction

Fig. 8a depicts the soil temperatures at different depths in the 3 zones during the period of monitoring from August 2009 to July 2010. There is no notable difference between zone A and zone B. The variations in zone C are slightly larger, which is normal because zone C has no protection by the ballast layer. For all the three zones, the lowest temperature was recorded in the period from December 2009 to February 2010, and is around 3 °C, higher than zero. This suggests that the line at this site is out of the freeze/thaw hazards. Longer recording is needed to confirm this conclusion.

Fig. 8b compares the soil surface temperature with the air temperature recorded by the weather station. There is quite little difference between them, but the fluctuation seems larger for the air temperature. In winter, the temperature decreased down to −10 °C. This suggests that the soil in the near ground surface level can undergo freezing if it is not covered by the ballast layer.

Fig. 9 depicts the evolutions of the air parameters measured by the weather station, including air temperature (Fig. 9a), solar radiation (Fig. 9b), wind speed (Fig. 9c), relative humidity (Fig. 9d) and precipitation (Fig. 9e). Note that due to a technical problem, the monitoring of relative humidity was interrupted in the beginning and in the middle of the recording period. It appears that the solar radiation directly conditions the air temperature: in winter the solar radiation is low giving rise to low air temperatures, whereas in summer the solar radiation is higher generating higher temperatures. For the wind speed, it appears that there are few differences from one season to another, except the exceptional wind recoded in early November 2009 at a speed close to 12 m/s. The variations of relative humidity are more pronounced in the period from March to July 2010 than in the period from September to December 2009. This is consistent with the precipitation. Indeed, there were more strong rainfalls in the second period that in the first (see Fig. 9e). Note that all data presented in Fig. 9 correspond to a recording frequency of 30 min.

The air data presented in Fig. 9 can be used to determine the potential evaporation rate using the model of Penman–Monteith (Allen et al., 1998):

$$ET_0 = \frac{0.408\Delta(R_n - G) + \gamma \frac{900}{T+273} u_2 (e_s - e_a)}{\Delta + \gamma(1 + 0.34u_2)} \quad (1)$$

where ET_0 is the potential evaporation (mm day^{-1}); R_n is the net solar radiation (MJ m^{-2} day^{-1}); G is the soil heat flux (MJ m^{-2} day^{-1}); T is the daily average temperature at 2 m above the ground surface (°C); u_2 is the wind speed at 2 m above the ground surface (m s^{-1}); e_s is the saturated vapour pressure (kPa); e_a is the actual vapour pressure that can be deduced from the air relative humidity using Kelvin's law (kPa); Δ is the slope of the curve of saturated vapour pressure versus temperature (kPa °C^{-1}); γ is the psychometric constant (kPa °C^{-1}).

As mentioned before, the measurements of air relative humidity were not complete in the monitoring period. Thereby, the data recorded in a Météo France weather station in Cambrai (close to the Moulin Blanc site) were used in the calculation. Fig. 10a shows the variations of ET_0 over the monitoring period. It appears clearly that the value of ET_0 is large in summer and small even equal to zero in winter, in agreement with the variations of solar radiation and air temperature shown in Fig. 9.

Fig. 10b shows the variations of suction in the three zones and at different depths. Again, because of the technical recording problem mentioned previously, the data are not complete and only the period from September to December 2009 and the period from April to July 2010 are covered. From the limited available data, it appears

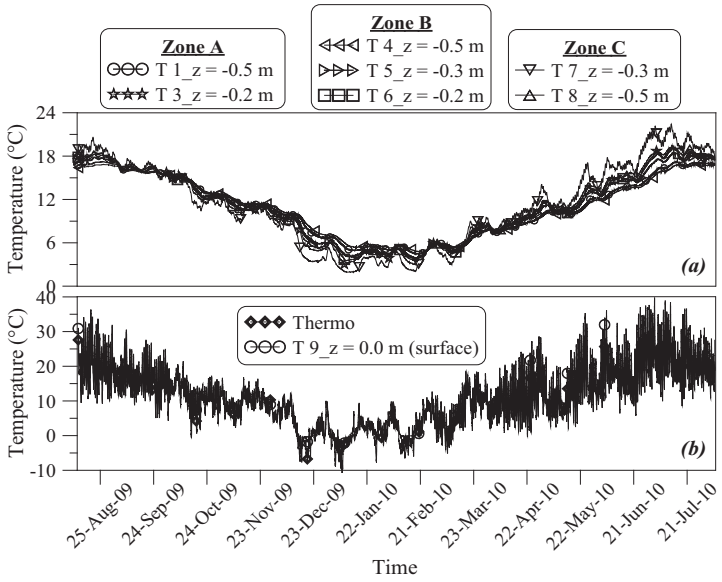

Fig. 8. Air and soil temperatures. (a) Soil temperatures in deferent zones and at different depths; (b) air temperature and soil surface temperature.

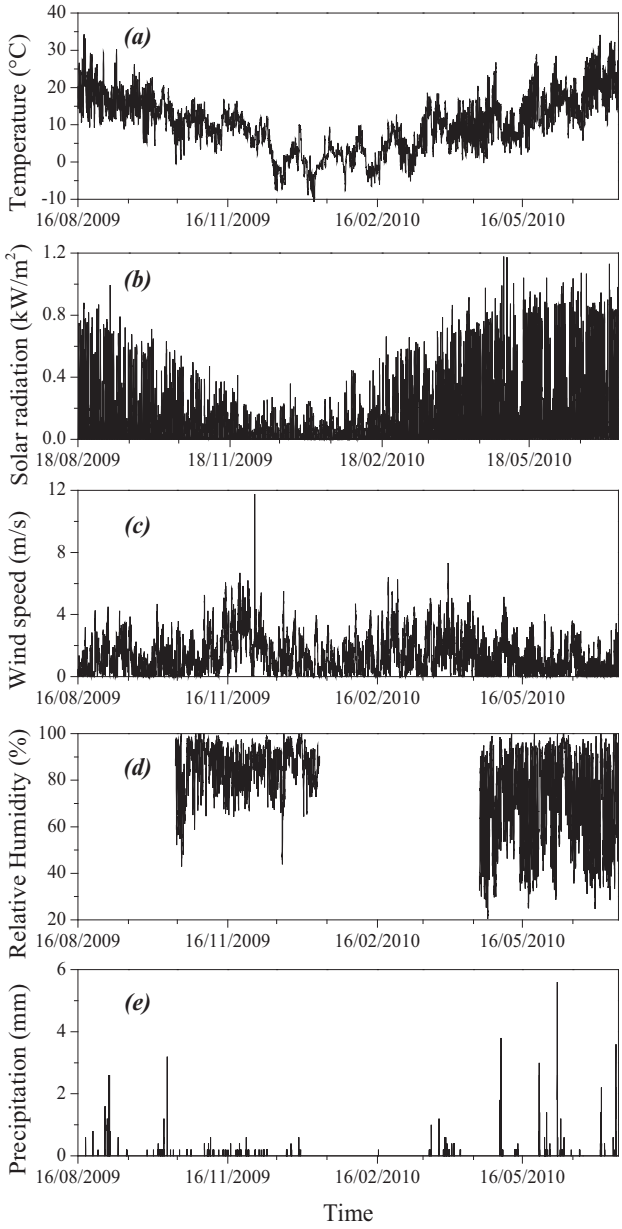

Fig. 9. Air data. (a) Temperature; (b) solar radiation; (c) wind speed; (d) relative humidity; (e) precipitation.

that in the relatively cold season (from September to December 2009), the suction values remained stable and small in all the three zones. By contrast, in the hot season (from April to July 2010), the values in zone A and zone B still remained stable but showed large variations in zone C. The difference between zone A/zone B and zone C is to be attributed to the effect of ballast layer.

Fig. 10c shows the daily precipitation in the monitoring period. The difference between this figure and Fig. 9e is that the former corresponds to a frequency of every day (precipitation amount for each day) whilst the latter corresponds to a frequency of every 30 min (precipitation amount for every 30 min). It can be observed that adopting a different frequency significantly changes the precipitation distribution feature: more details can be found with a high frequency (30 min) while the precipitation values are more averaged in the case of low frequency (one day). It appears in Fig. 10c that the strong rainfall events occurred in the period from April to July 2010. This suggests that the large variations of suction identified in zone C in this period (see Fig. 10b) are not related to the rainfalls, but to the high water evaporation rate. In other words, at the site of Moulin Blanc in the monitoring period the evaporation rate was larger than the water infiltration rate in the zone out of tracks – the soil was being dried over time. This explains why no water table was detected

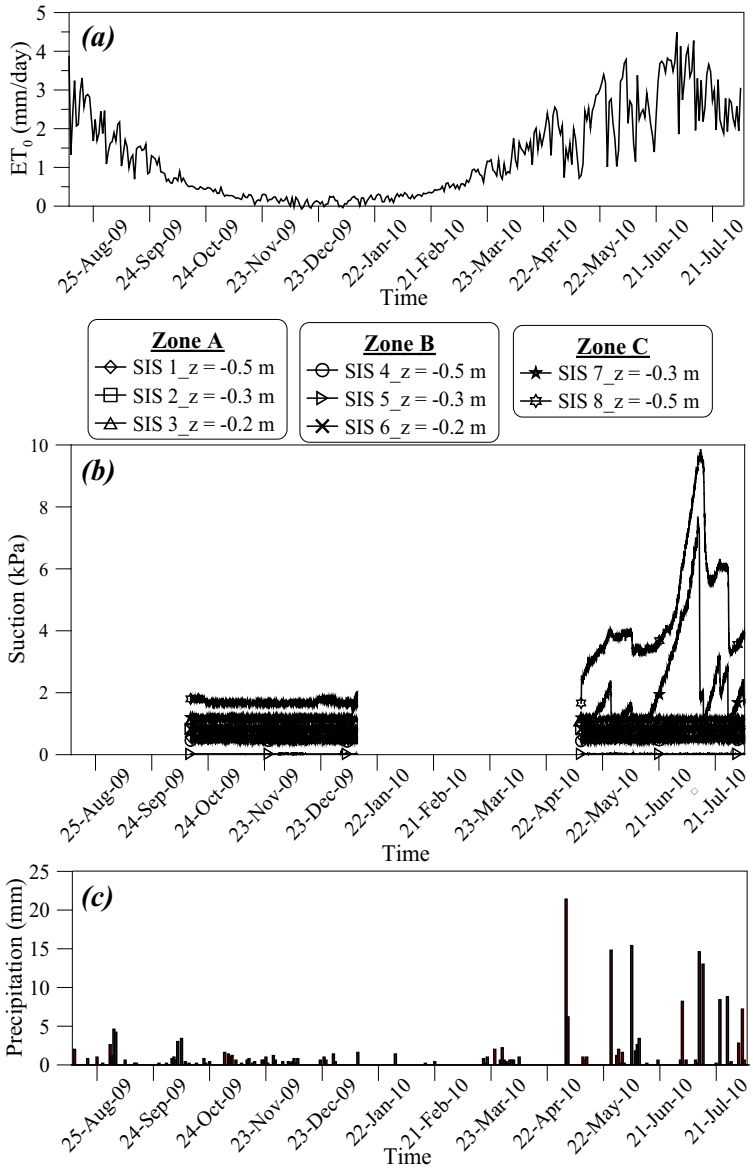

Fig. 10. Potential evaporation (a), suction (b) and daily rainfall (c).

by the two piezometres installed till 10 m depth. Further examination shows that under the ballast layer (zones A and B) suction did not change, indicating the effective protection of the ballast layer against water evaporation on one hand and water infiltration on the other hand.

Acceleration and assessment of the double integration method

As mentioned before, strain gauges were glued on rails to measure the rail strain under the effect of train circulation. The recorded data can be used to differentiate the train types and determine their axle weight and number of axles, provided a calibration was undertaken allowing relating the weight applied to the rail strain recorded. Then, the types of train can be differentiated by the 'signatures' of their passages (Fig. 11). Thereby, a 18-coach TGV train (300 m long) in Fig. 11a, a 3-coach TER train (50 m long) in Fig. 11b and a 23-wagon freight train (430 m long) in Fig. 11c can be identified. Moreover, for each kind of train, the axle weight can be determined and empty or loaded coach can be identified. For instance, In Fig. 11c, five empty coaches behind the locomotive are observed for the freight. Comparison of the weight per axle between the three types of train involved shows that the TGV train and TER train have similar weight per axle (around 15 Mg depending on the passengers' load) while Freight train has a weight per axle much larger, up to 22.5 Mg.

The vibration produced by a train within the railway platform depends on the weight per axle, the geometry

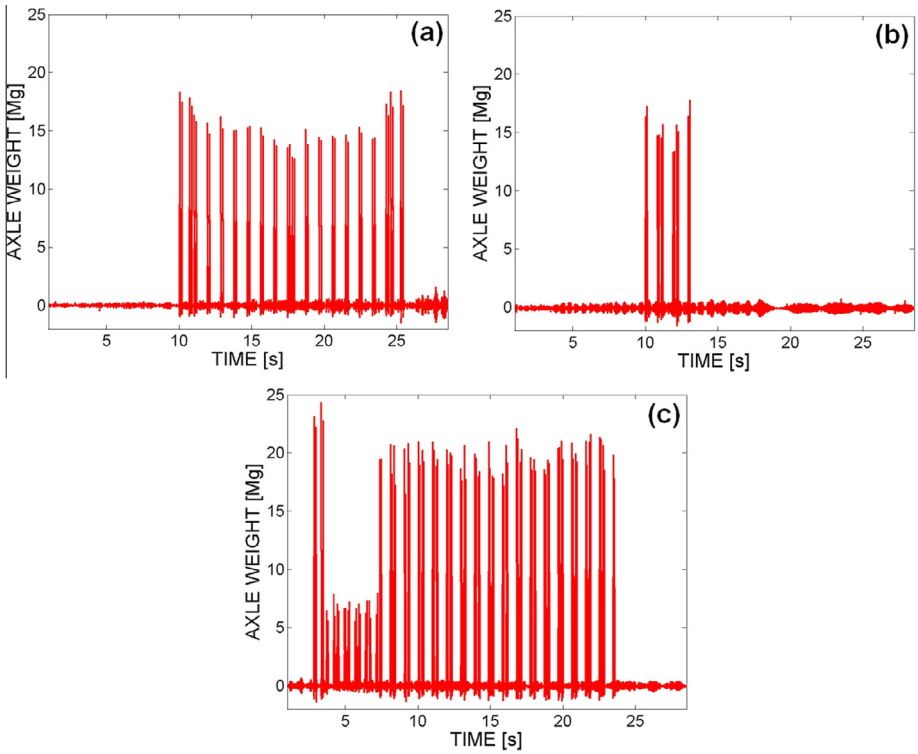

Fig. 11. Axle weight for different trains (a) TGV (passengers); (b) TER (passengers); (c) Freight train.

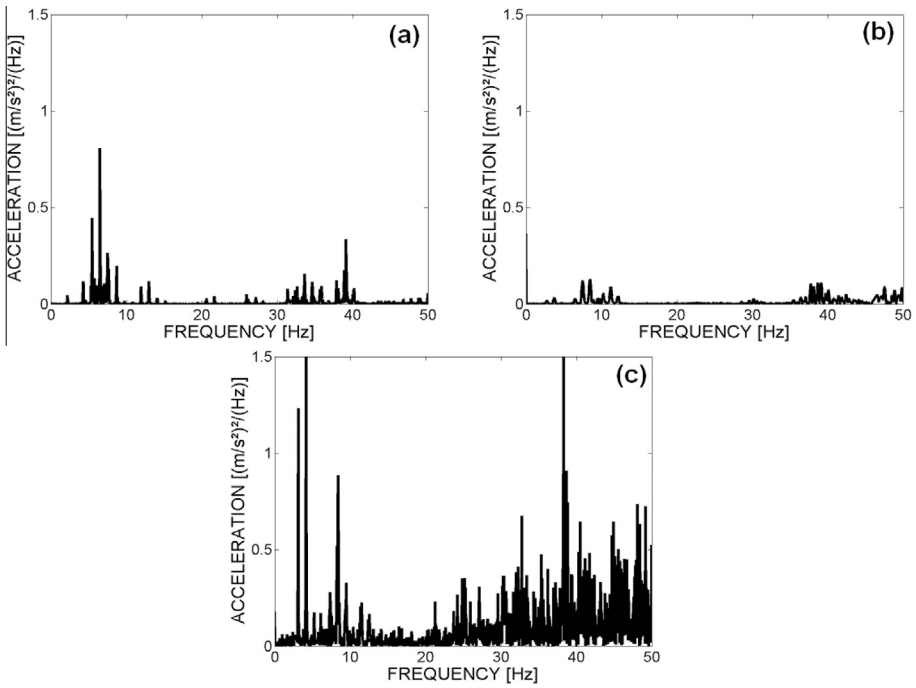

Fig. 12. Power spectrum density (0–50 Hz) for a train at 80 km/h. (a) TGV; (b) TER; (c) Freight.

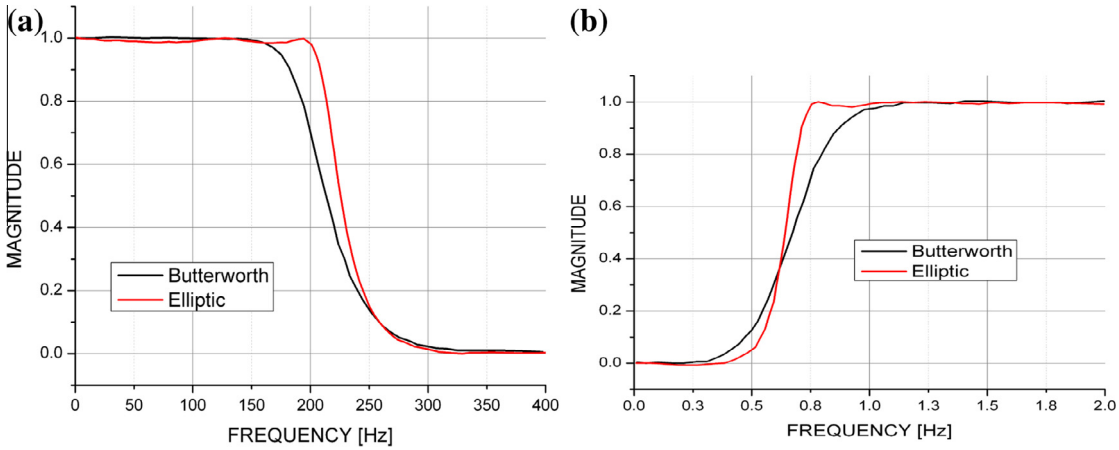

Fig. 13. Filters adopted. (a) >200 Hz; (b) <0.75 Hz.

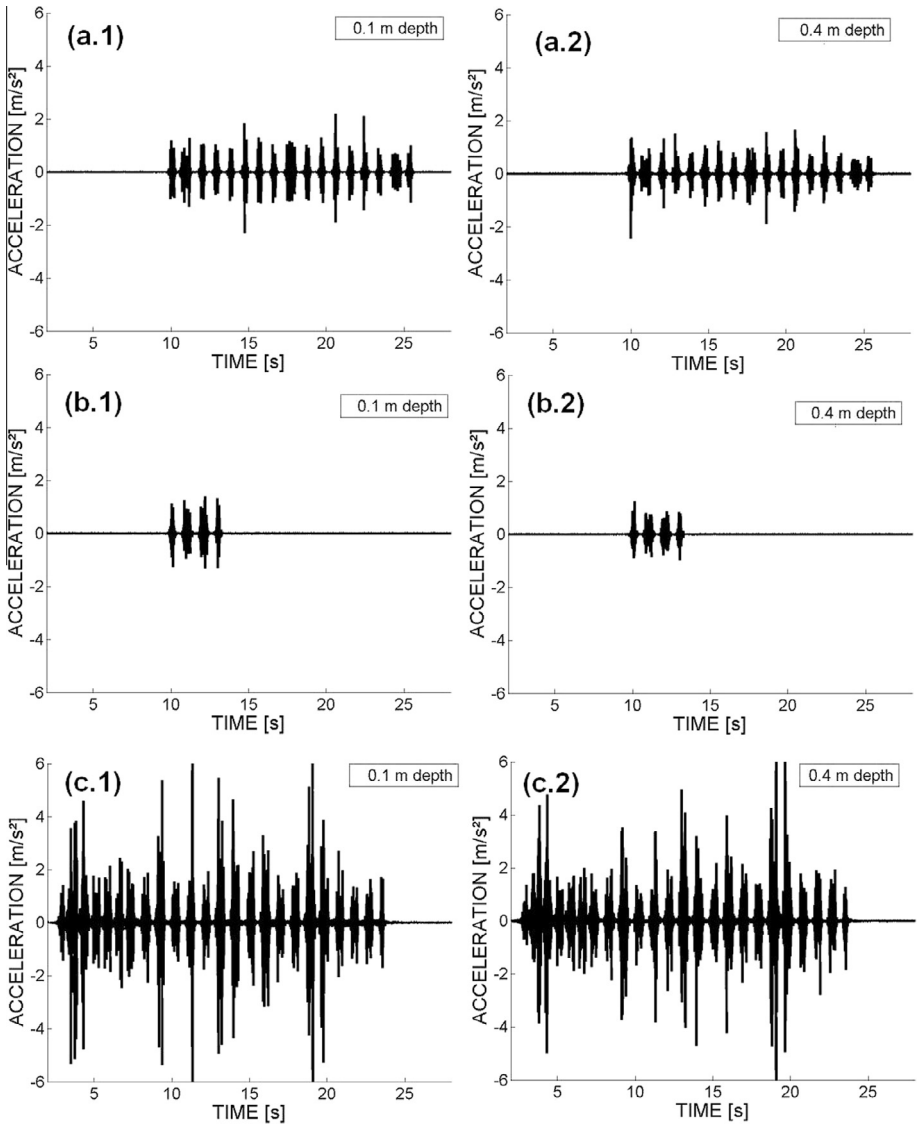

Fig. 14. Particles accelerations induced by different trains running at 80 km/h filtered with an elliptic filter. (a) TGV (b) TER (c) Freight. (1) −0.1 m under the ballast layer (2) −0.4 m under the ballast layer.

of train, the train velocity as well as the platform's properties. In general, the signals of high energy content are those at low frequencies. The monitoring of this kind of low-frequency signals requires the use of accelerometers with good accuracy. From the records of accelerometers, the variations of power spectrum density (PSD) which describes how the power of the signal is distributed with frequency can be determined for the passage of a train. Fig. 12 shows such variations determined based on the records of the accelerometer installed at −0.10 m depth below the ballast layer, in the range of frequency from 0 to 50 Hz for the three types of train running at 80 km/h. Note that in the determination, a time interval of 30 s was considered. The energy content of the TER acceleration signal is found relatively low. This can be explained by its low weight and its short length. As a train at a given velocity can excite the platform in different frequencies due to the different wavelengths (Kleinert, 2001) related to the whole railway system, the power spectrum density presents various peaks corresponding to the different wavelengths. From the variations of PSD, it is possible to distinguish the contributions of different elements of the railway system. For instance, in Fig. 12a for TGV, the density or energy content in the low frequency range from 0 to 10 Hz corresponds to wagon, bogie and axle wavelengths. This part of energy is much higher than that in the range of higher frequency (>10 Hz). Furthermore, in the range of low frequency, the inter-bogie frequency (about 6 Hz) and the inter-axle frequency (about 8 Hz) can be distinguished. The peak at about 40 Hz corresponds to the track sleepers spacing (0.60 m).

The records of accelerometers can also be used to estimate the particle velocity and displacement using the

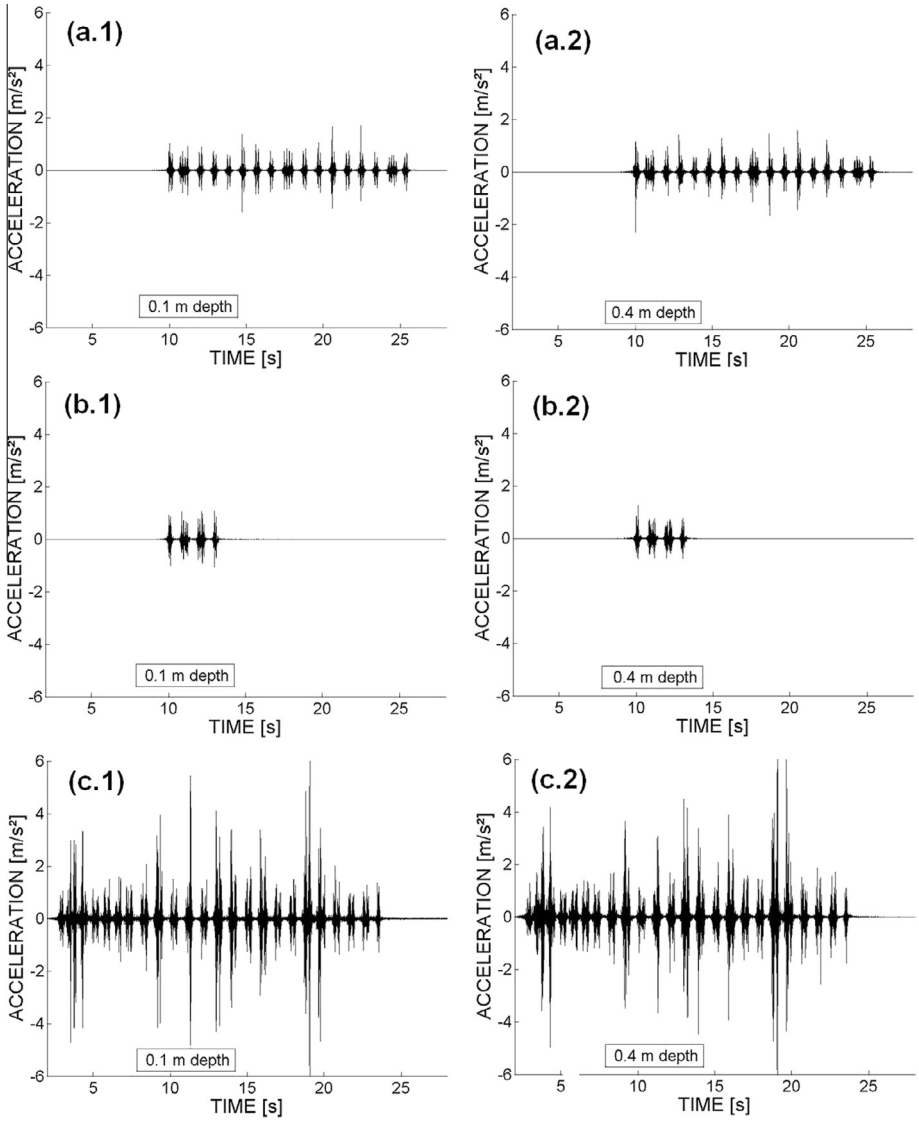

Fig. 15. Particles accelerations induced by different trains running at 80 km/h filtered with a Butterworth filter. (a) TGV (b) TER (c) Freight. (1) −0.1 m under the ballast layer (2) −0.4 m under the ballast layer.

double integration method by following a trapezoidal rule as proposed by Zuada–Coelho (Zuada-Coelho, 2011):

$$v(n) = v(n-1) + \frac{\Delta t}{2}[a(n) + a(n-1)] \quad (2)$$

$$d(n) = d(n-1) + \frac{\Delta t}{2}[v(n) + v(n-1)] \quad (3)$$

where $v(n)$ and $d(n)$ are respectively the first integration (velocity) and the second integration (displacement) of the discrete acceleration signal $a(n)$.

As the piezo-electric accelerometers used in this study cannot operate for a frequency lower than 0.47 Hz, it is then necessary to apply a high-pass filter to the recorded acceleration data in order to avoid a baseline error after the integration of the signal (Boore, 1999; Boore et al., 2002), because after an integration of the signal the low frequencies are magnified and the high frequencies are reduced. Any constant or slow variation of the signal (in the very low frequency range) controls the results of the displacement obtained by the double-integration method. Moreover, it is necessary to eliminate the part of signal corresponding to the frequencies higher than 200 Hz. These frequencies are due to the defects of the wheel (with a wavelength from 1 to 5 cm) and of the rail (with a wavelength smaller than 10 cm). As mentioned above, these frequencies do not affect the amplitude of displacement calculated. A low-pass filter is needed for the part related to the high frequencies.

In this study, two filter methods are adopted: the Butterworth method and the elliptic method (SNCF Research and Development, 2011). The cut-off frequency for the low-pass filters is 200 Hz, while the cut-off frequency for the high-pass filters is 0.75 Hz to ensure that all signals for the frequencies lowers than 0.47 Hz does not influence the calculations. For both high and low pass elliptic filters,

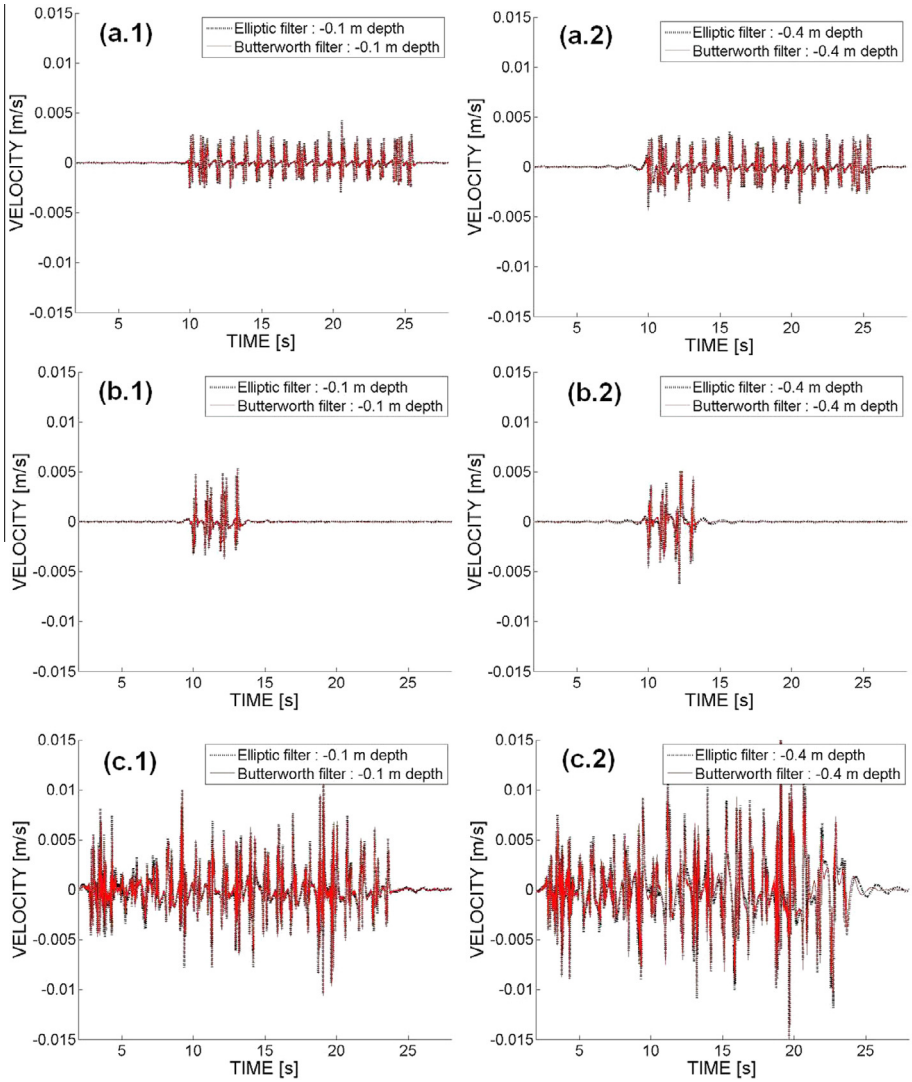

Fig. 16. Particle velocities induced by different trains running at 80 km/h filtered with elliptic and Butterworth filters. (a) TGV (b) TER (c) Freight. (1) −0.1 m under the interlayer soil (2) −0.4 m under the interlayer soil.

the pass-band ripple is taken equal to 0.1 dB and the stop-band attenuation equal to 60 dB. Fig. 13 presents the filtering magnitude factor applied to the signals according to the excited frequency for each used filter method. This magnitude factor is the factor which multiplies the value of the signal at each frequency. It appears that the elliptic method gives better results than the Butterworth method in terms of frequency cut-off values.

Fig. 14 shows the acceleration data recorded at two depths (−0.10 and −0.40 m under the ballast layer) and filtered with an elliptic filter for TGV train (Fig. 14a), TER train (Fig. 14b) and Freight train (Fig. 14c). As expected, a decrease of amplitude of acceleration is observed from −0.10 to −0.40 m depth for both TGV and TER trains. However this decrease is not notable for the freight train, showing a clear effect due to the weight per axle. The observed decrease is mainly related to the load transmission and wave radiation. The same acceleration data filtered with a Butterworth filter are shown in Fig. 15, for TGV train (Fig. 15a), TER train (Fig. 15b) and Freight train (Fig. 15c). Comparison between Figs. 14 and 15 shows that the amplitudes of the signals filtered with an elliptic filter are slightly greater than those with a Butterworth filter. This can be explained by the form of each filter shown in Fig. 13.

Application of the first integration of the filtered acceleration data gives the particle velocity, as shown in Fig. 16 for the three different trains and at two different depths under the ballast layer. Note that the amplitudes of the first integration of the acceleration signals are dominated

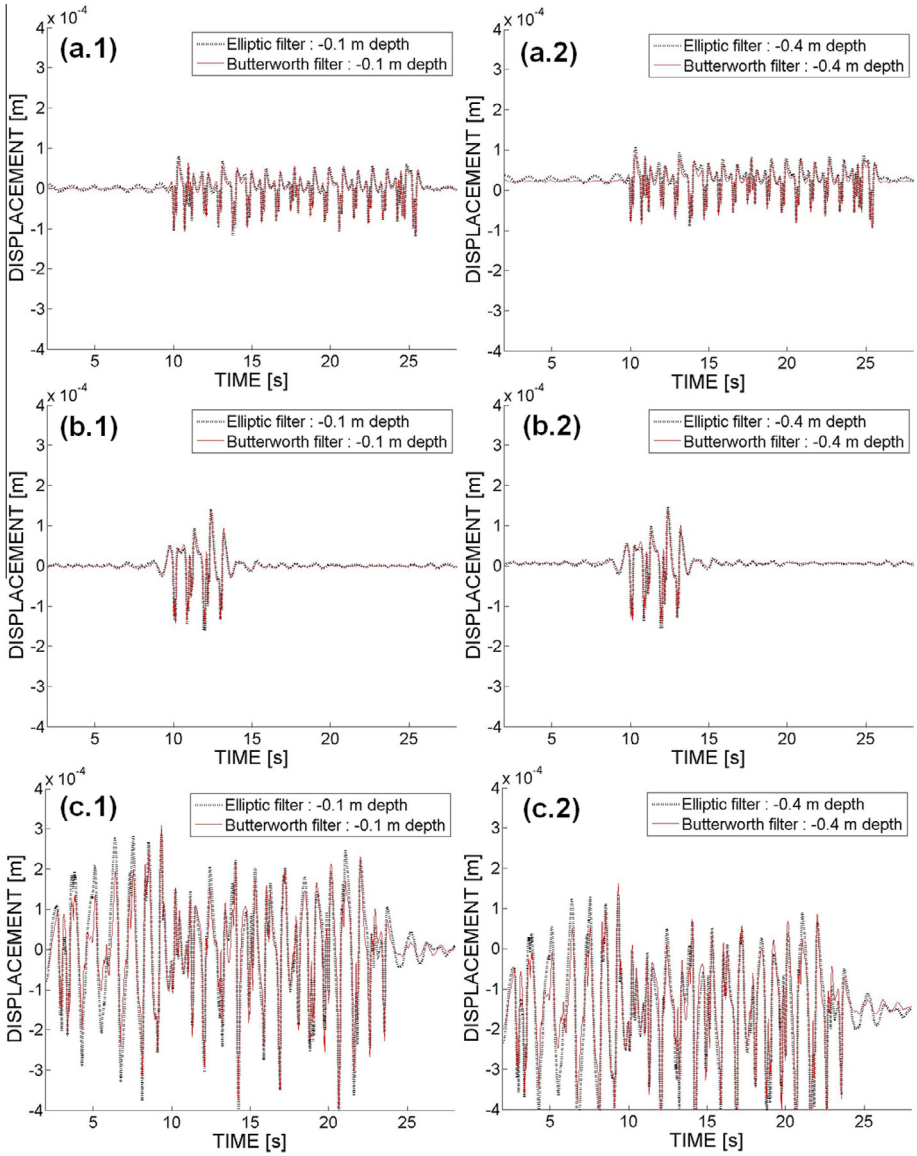

Fig. 17. Particle displacements induced by different trains running at 80 km/h filtered with elliptic and Butterworth filters. (a) TGV (b) TER (c) Freight. (1) −0.1 m under the ballast layer (2) −0.4 m under the ballast layer.

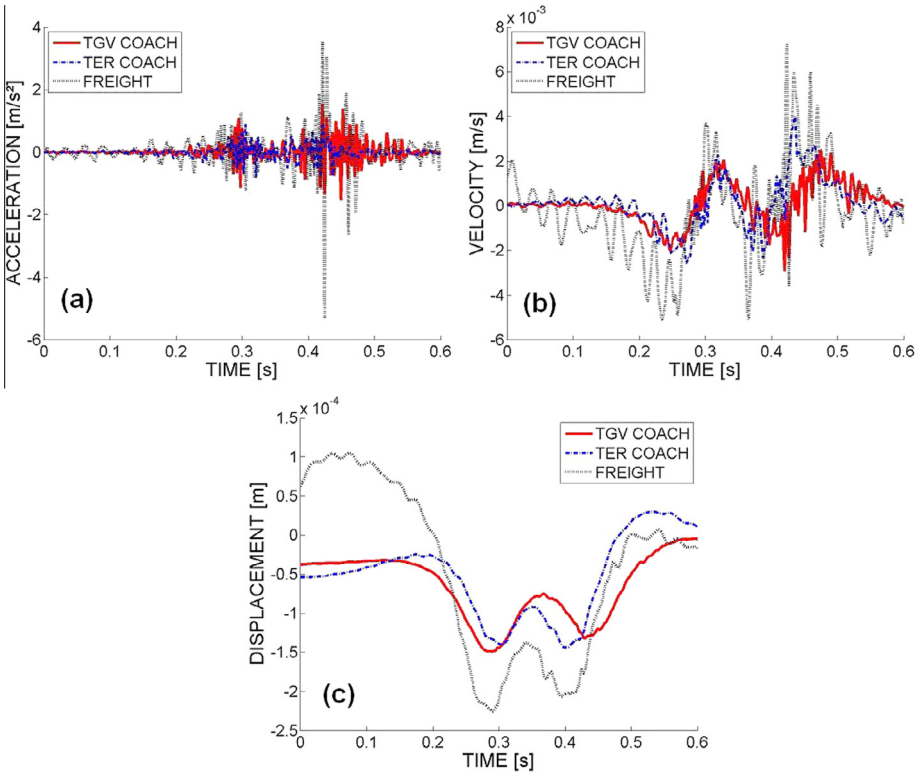

Fig. 18. Comparison between the effects of different train bogies (TGV, TER and Freight) at 80 km/h for the −0.1 m depth under the ballast layer. (a) Particle acceleration (b) Particle velocity (c) Particle displacement.

by the low-mid frequencies (0–100 Hz). Even though the acceleration amplitudes are similar for TGV and TER (see Figs. 14 and 15), the particle velocity in the case of TER is larger than in the case of TGV. This can be explained as follows: although the weight per axle is similar for both trains, the excitations are different because of the difference in length. The TER train is about 6 times shorter than the TGV and 9 times shorter than the freight one. Normally, higher frequencies can be expected in the case of shorter trains. As expected, the freight train led to the largest particle velocity among the three types of train. Moreover, as opposed to the results for the TGV and TER trains which are more homogeneous due to the homogeneity in weight per axle, the results for the freight train shows larger variability due to the heterogeneity in weight per axle.

Comparison between the amplitudes at the two different depths shows that the values are similar for TGV and TER. By contrast, the values at −0.40 m depth is much lower than those at −0.10 m in the case of freight. This suggests that the interlayer of conventional lines helps dissipate the energy corresponding to the mid frequency loads. The difference between the elliptic filter and the Butterworth filter is not notable. This is because there is not much difference between both filters in the range of mid frequency that governs the response in particle velocity.

Prior to processing the second integration, it is necessary to apply the filters once again to avoid the baseline correction error. After the second integration, the particle displacement can be obtained. Fig. 17 shows the obtained results for the three types of train and at two different depths. As the particle velocity, the particle displacement in the case of TER is also larger than that in the case of TGV, the particle displacement in the case of freight being the largest. Comparison of the values between the two depths in each case shows that they are similar in the cases of TGV and TER, but the values at −0.40 m are slightly lower than those at −0.10 m. As for the particle velocity, the difference between the elliptic filter and the Butterworth filter is not notable.

If we focus on one bogie of each train, it is possible to compare the results for different trains at a given depth. For this purpose, the responses at −0.10 m depth to the excitation of a TGV engine bogie (mean axle weight of 16 Mg), a TER bogie (mean axle weight of 15.8 Mg) and a full wagon of a freight (axle weight of 22.5 Mg) are compared and shown in Fig. 18. As the mean axle weight of a TGV coach is similar to that of a TER coach, the responses are quite similar in terms of particle acceleration, velocity and displacement. By contrast, for a fully loaded freight wagon, the particle acceleration, velocity and displacement are much larger.

Conclusions

In order to better understand the hydro-mechanical behaviour of the interlayer soil naturally formed in the

platform of the conventional lines in France, field monitoring was undertaken at the Moulin Blanc site. The parameters monitored include climatic data, soil suction, soil temperature, water table and particle accelerations. The recorded data allowed the thermal and hydric behaviours of the platform to be analysed on one hand, and on the other hand the double integration method for the particle velocity and displacement to be assessed. The following conclusions can be drawn:

The temperature under the ballast layer remained positive even though the temperature outside was as low as −10 °C, suggesting that the investigated site is out of freeze/thaw hazards. Note that longer monitoring is needed to confirm this observation.

The suction under the ballast layer remained low and unchanged over the monitoring period. However, significant changes were recorded in the zone where the soil ground is directly exposed to the atmosphere without being covered by ballast. These changes were mainly due to water evaporation. Comparison between the potential evaporation rate and the precipitation showed that the site was in deficiency in water supply. This explained the absence of water table till the depth (10 m) of the installed piezometres.

The double integration method can be used to successfully determine the particle velocity and particle displacement from the recorded particle acceleration, provided that appropriate filters such as elliptic filter and Butterworth filter are used to eliminate the low-frequency values related to the accuracy of employed accelerometers and the high frequency values related to the defects of wheels, rails, etc. The elliptic filter has been found to give better cut-off values of frequency than the Butterworth filter.

Three types of train were considered, TGV, TER and Freight. The axel weights of TGV and TER are similar. The particle accelerations of the two types of train are also similar, but the particle velocity and particle displacement are larger in the case of TER. For the Freight, because of its heavy axel, the particle acceleration, velocity and displacement are the greatest among the three types of trains.

As far as the responses at different depths are concerned, it has been found that there is few difference in the cases of TGV and TER, especially in terms of particle velocity and particle displacement. But a significant decrease with depth was identified in the case of Freight.

Note that even though interesting results have been obtained using the double integration method, further work must be conducted to confirm these results. The future work mainly involves the field monitoring of soil displacements.

References

Allen RG, Pereira LS, Raes D, Smith M, Crop evapotranspiration – Guidelines for computing crop water requirements. FAO – Food and Agriculture Organization of the United Nations paper, 1998;56:p.300.

Boore DM. Effect of baseline corrections on displacements and response spectra for several recordings of the Chi-Chi, Taiwan earthquake. Bull Seismol Soc Am 1999;91(2001):1199–211.

Boore DM, Stephens CD, Joyner WB. Comments on baseline correction of digital strong-motion data: examples from the 1999 Hector Mine, California, earthquake. Bull Seismol Soc Am 2002;92:1543–60.

Cui YJ, Duongt TV, Tang AM, Dupla JC, Calon N, Robinet A. Investigation of the hydro-mechanical behavior of fouled ballast. J Zhejiang Univ Sci A 2013;144(4):244–55.

Duongt TV, Trinh VN, Cui YJ, Tang AM, Calon N. Development of a large-scale infiltration column for studying the hydrauli behavior of fouled ballast. Geotech Test J 2013;36(1):54–63.

Duongt TV et al. Effects of fines and water contents on the mechanical behaviour of interlayer soil in ancient railway sub-structure. Accepted for a publication in Soils and Foundations, 2013.

Müller-Boruttau U. Kleinert. Concrete sleepers with sole pads – experiences and findings with a new type of track component. ETR – Eisenbahntechnische Rundschau;2001;vol. 3:p. 90–98.

SNCF Direction de l'Ingénierie. IN 3278: Référentiel technique pour la réalisation des LGV – partie Génie Civil. Référentiel Infrastructure SNCF, 2006.

SNCF Research & Development, DYNAE/SNCF: Assistance à la réalisation des filtres numériques. Internal report, 2011.

Trinh VN et al. Mechanical characterization of the fouled ballast in ancient railway track substructure by large-scale triaxial tests. Soil Found 2012;52(3):511–23.

Trinh VN et al. Caractérisation des matériaux constitutifs de plate-forme ferroviaire ancienne. Revue Française de Géotechnique 2011;134–135:65–74.

Zuada-Coelho BE, Dynamics of railway transition zones in soft soils. PhD Thesis, Technische Universiteit Delft, 2011.